Dynamical Clustering and Phase Separation in Suspensions of Self-Propelled Colloidal Particles

Ivo Buttinoni,[1] Julian Bialké,[2] Felix Kümmel,[1] Hartmut Löwen,[2] Clemens Bechinger,[1,3] and Thomas Speck[2]

[1]II. Institut für Physik, Universität Stuttgart, D-70569 Stuttgart, Germany
[2]Institut für Theoretische Physik II, Heinrich-Heine-Universität, D-40225 Düsseldorf, Germany
[3]Max-Planck-Institute for Intelligent Systems, D-70569 Stuttgart, Germany

We study experimentally and numerically a (quasi-)two-dimensional colloidal suspension of self-propelled spherical particles. The particles are carbon-coated Janus particles, which are propelled due to diffusiophoresis in a near-critical water-lutidine mixture. At low densities, we find that the driving stabilizes small clusters. At higher densities, the suspension undergoes a phase separation into large clusters and a dilute gas phase. The same qualitative behavior is observed in simulations of a minimal model for repulsive self-propelled particles lacking any alignment interactions. The observed behavior is rationalized in terms of a dynamical instability due to the self-trapping of self-propelled particles.

Following our physical intuition, "agitating" a system by, e.g., increasing the temperature also increases disorder. The most simple and paradigmatic example is the Ising model of interacting spins on a lattice, which, in two or more dimensions, displays a second-order phase transition from an ordered state to a disordered state as we increase the temperature [1]. Nonequilibrium driven systems, however, may defy our intuition and show the opposite behavior: increasing the noise strength leads to the emergence of an ordered state [2,3], for example the "freezing by heating" transition of oppositely driven particles in a narrow channel [4].

Self-propelled, or "active" particles are one class of nonequilibrium systems that currently receives considerable attention [5–13]. These are model systems for "living active matter" ranging from microtubules [14] to dense bacterial solutions [15–17], to flocks of birds [18]. A common feature of many of these models is that the particle orientations align, which leads to a multitude of collective phenomena such as swarming [19] and even microbacterial turbulence [20]. This alignment interaction can be either explicit (Vicsek-type models [21]) or indirect. For example, in dense granular systems of rods [22] and disks [23], the combination of hard-core repulsion and propulsion implies an effective alignment. Somewhat surprisingly, recently it has been found that also self-propelled suspensions lacking any alignment mechanism are able to show collective behavior. Specifically, simulations of a minimal model for a suspension of repulsive disks below the freezing transition [24] show phase separation into a dense large cluster and a dilute gas phase [25,26]. Phase separation due to a density-dependent mobility has been discussed theoretically in the context of run-and-tumble bacteria [27], and a link has been made recently to self-propelled Brownian particles [28].

Experimentally, active clustering of spherical colloidal particles has been observed for sedimenting, platinum-coated gold particles [10] and colloidal particles with an embedded hematite cube [13], where platinum and hematite act as catalysts for the decomposition of water peroxide. In both studies, aggregation is attributed to attractive forces. In this Letter, we investigate a suspension of carbon-coated colloidal Janus particles dispersed in a near-critical mixture of water and lutidine. This setup allows us to continuously vary the propulsion speed by changing the illumination power [11]. We have chosen material and experimental conditions at which the influence of attractions—due to van der Waals forces and the phoretic motion—is largely reduced. Instead, the clustering is caused by dynamical self-trapping of the self-propelled particles. This mechanism is generic and does not depend on the actual means of propulsion. At higher densities (but still below the freezing transition), we report the first experimental data for active colloidal suspensions showing phase separation, whereby clusters grow to a finite fraction of the system size. The robustness of this transition is qualitatively confirmed in simulations of purely repulsive disks.

Janus particles are prepared from SiO_2 beads with a radius of $R \simeq 2.13$ μm by sputtering a thin layer (10 nm) of graphite onto one hemisphere. These carbon-coated particles are then suspended in a water-2,6-lutidine mixture close to the critical concentration (28 mass% lutidine) and a small amount of suspension is poured in a 400×400 μm^2 cavity. The cavity is made by photolithography of SU-8 photoresist on a glass surface. The 2D area fraction ϕ is tuned up to 0.4 by adjusting the concentration of the initial suspension. The sample is sealed with a cover glass on top. Since the height of the cavity is about 6 μm, the motion of the particles is confined to quasi-2D although the spheres remain free to rotate in 3D.

The propulsion mechanism [11,12] is summarized as follows: The active motion is obtained by illuminating the entire sample with a widened laser beam with wavelength 532 nm. The laser light is absorbed by the carbon-coated hemisphere, which locally heats up the binary

solvent above the critical temperature. The ensuing demixing provides a phoretic force that propels the particles since the two hemispheres possess different surface properties with respect to water and lutidine. Unlike catalytic swimmers [29], e.g., particles propelled in a H_2O_2 solution [5,6,10,13] where the molecular solute is "consumed" by the chemical reaction, in the setup used here the environment is not affected by the local demixing due to the reversibility of the spinodal decomposition. Employed illumination intensities (≤ 5 μW/μm^2) are weak compared to values reported previously on thermophoretic motion of colloidal Janus particles [8]. Moreover, particle motion is Brownian far below the critical temperature of the water-lutidine mixture even with the illumination turned on. Hence, we conclude that thermophoretic effects are negligible and that diffusiophoresis is the principal propulsion mechanism [12].

The axis joining the poles of the two hemispheres defines the particle orientation along which it is propelled. Particle motion in dilute suspensions is described by a persistent random walk [11,12]. The measured mean-square displacement follows the expression [7]

$$\langle \Delta r^2 \rangle = 4D_0 t + \frac{v^2}{2D_r^2}[2D_r t + e^{-2D_r t} - 1], \qquad (1)$$

where $D_0 \simeq 0.029$ μm^2/s is the bare diffusion coefficient measured in equilibrium, v is the swimming speed, and D_r is the rotational diffusion coefficient. The latter, as obtained from fits, is independent of v and approximately obeys the no-slip relation $D_r \approx 3D_0/(2R)^2$ between translational and rotational diffusion coefficient, showing that particles undergo free rotational diffusion. In the following, the control parameters are the area fraction ϕ and the laser intensity. In order to estimate the swimming speed v in dense suspensions for a given intensity, we determine the trajectories of isolated particles and fit their short-time mean-square displacement to the expansion $4D_0 t + (vt)^2$ of Eq. (1).

Under equilibrium conditions, i.e., with the illumination turned off, we observe a homogeneous suspension at all studied area fractions $\phi \simeq 0.1$–0.4. After turning on the illumination, the particles are driven out of thermal equilibrium and are propelled along their orientation. We let the system relax into a steady state (for about 15 minutes) and then analyze trajectories with a length of about 5 minutes. Typical situations at low and high density are presented in Fig. 1. At low densities, the system indeed rapidly enters a steady state that can be described as a dynamical cluster fluid. Figure 1(a) shows the temporal evolution of a small cluster. It clearly demonstrates that the aggregation is dynamical; i.e., particles join and leave the cluster, until in the last snapshot the cluster has finally broken into two smaller clusters. Figure 1(b) shows that the mean cluster size increases approximately linearly as a function of the propulsion speed similar to what has been observed by Theurkauff *et al.* [10].
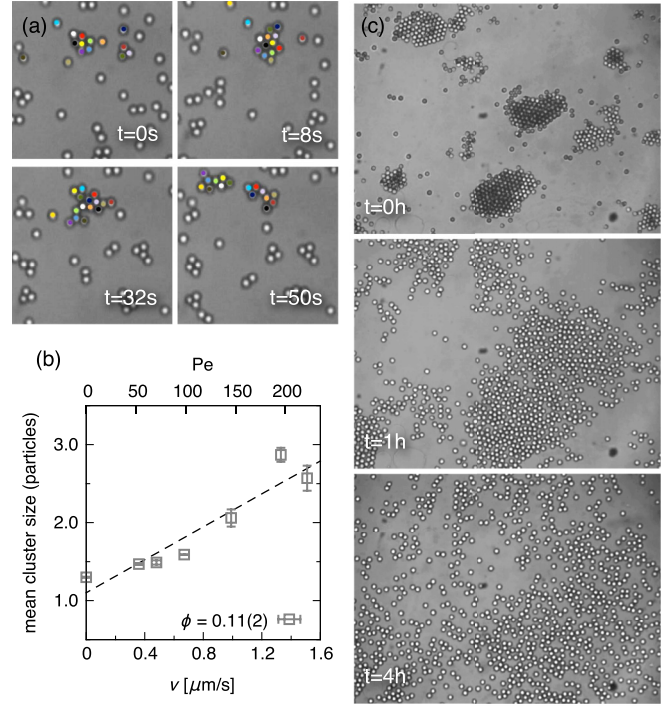

FIG. 1 (color online). (a) Dynamical clustering of self-propelled colloidal particles at low densities ($\phi \simeq 0.1$ and $v \simeq 0.65$ μm/s). Shown is the formation and breaking up of one cluster. Every particle that at one time has been a member of the cluster is colored differently. (b) The mean cluster size increases linearly as a function of speed v. The dashed line is the fit $1.1 + 1.1v$. Error bars indicate the statistical uncertainty. (c) At higher densities ($\phi \simeq 0.27$ and $v \simeq 1.63$ μm/s), phase separation into a few big clusters and a dilute phase occurs. The aggregation is completely reversible: The snapshots show how the clusters dissolve after the illumination has been turned off.

At higher densities, we observe a phase separation [cf. Fig. 1(c)] where clusters grow until the system consists of a few big clusters surrounded by a dilute gas phase. We presume that the final stage is the condensation into one cluster. However, the slow dynamics of the large aggregates puts the direct observation of this final stage out of our current reach. Figure 1(c) shows the temporal evolution of the sample after we turn off the illumination. Particle diffusion restores the homogeneous density profile, indicating that also for large clusters the aggregation is reversible and solely induced by the propulsion of the colloidal particles.

We employ computer simulations of a minimal model [24–26] both in order to corroborate our experimental conclusions and to test the limits of simplified mathematical models applied to self-propelled suspensions. The model is defined as follows: We simulate $N = 4900$ interacting particles, each of which has an orientation $\mathbf{e}_k$ diffusing freely about the z axis with rotational diffusion coefficient D_r. Particles move in two dimensions in a quadratic box with periodic boundary conditions. In addition to translational

Brownian motion, particles are propelled along their orientation with a constant speed. Moreover, we neglect hydrodynamic interactions between colloidal particles. The coupled equations of motion are

$$\dot{\mathbf{r}}_k = -\nabla_k U + \text{Pe}\, \mathbf{e}_k + \boldsymbol{\xi}_k \qquad (2)$$

for the particle positions $\{\mathbf{r}_k\}$, where the Gaussian white noise $\boldsymbol{\xi}_k$ models the coupling to the solvent and $U = \sum_{k<k'} u(|\mathbf{r}_k - \mathbf{r}_{k'}|)$ is the potential energy due to pairwise interactions. Quantities are made dimensionless using $2R$ as the unit of length and $(2R)^2/D_0$ as the unit of time, which implies the Péclet number $\text{Pe} = 2Rv/D_0$. The equations of motion (2) are integrated with a (minimal) time step 10^{-5}.

The experiments are carried out in a quasi-two-dimensional geometry. Particles may move out of plane and slightly overlap in the recorded images. To account for this (apparent) softness in the simulations, for the pair interactions we choose

$$u(r) = \begin{cases} \varepsilon u_{\text{LJ}}(r) + u_{\text{LJ}}(2R)(\lambda - \varepsilon) & (r \le 2R) \\ \lambda u_{\text{LJ}}(r) & (r > 2R) \end{cases} \qquad (3)$$

with Lennard-Jones potential $u_{\text{LJ}}(r) = 4[(\sigma/r)^{12} - (\sigma/r)^6]$. That is, we use a repulsive core (the WCA potential) to which optionally we add an attractive tail of depth λ [30]. For the passive equilibrium system (no illumination), Fig. 2(a) compares the experimentally measured radial distribution function $g(r)$ with the simulation results, both at area fraction $\phi \simeq 0.37$. We fix $\varepsilon = 100k_BT$ and $\sigma/(2R) = 2^{-1/6} \simeq 0.891$ such that the potential minimum coincides with the particle diameter, see Fig. 2(b). Good agreement between experiment and simulations is achieved by adding a small attraction with $\lambda = 0.5k_BT$ in the simulations. However, in the following we will focus on the purely repulsive pair potential with $\lambda = 0$ to show that, conceptually, the observed phenomena do not depend on attractions.

Clusters are determined from a simple overlap criterion: In the simulations, all particles with a separation smaller than their diameter share a "bond." A cluster is then the set of all particles that are mutually bonded. For the experimental trajectories we use a slightly different method, where we estimate cluster sizes through the enclosed area since within larger clusters it becomes difficult to reliably detect particle positions. The measured mean cluster size in Fig. 1(b) increases linearly as a function of the speed; i.e., the driving stabilizes small clusters. As shown in Fig. 1(a), these clusters are dynamical and not the result of irreversible aggregation. The simulation results shown in Fig. 3(a) demonstrate that a purely repulsive pair potential is sufficient to reproduce the increase of the mean cluster size with swimming speed. However, comparing with Fig. 1(b), the increase of the cluster size is somewhat stronger in the experiments. The snapshots of the simulations [Fig. 3(b)] and experiments [Figs. 3(c) and 3(d)] reveal another difference: while in the simulations a few large clusters dominate, the experimental snapshots show many clusters containing fewer particles. These differences are most likely due to the influence of hydrodynamics, see also the Supplemental Material [31] for more details. Hydrodynamic aggregation of swimmers has been demonstrated in simulations [32] and experimentally [15,33].

Increasing the density, we observe a transition from the initially disordered, homogeneous fluid into an ordered state as we change the swimming speed, see Figs. 1(c) and 4(c). The ordered state is comprised of a few big clusters surrounded by a dilute phase of single self-propelled particles.
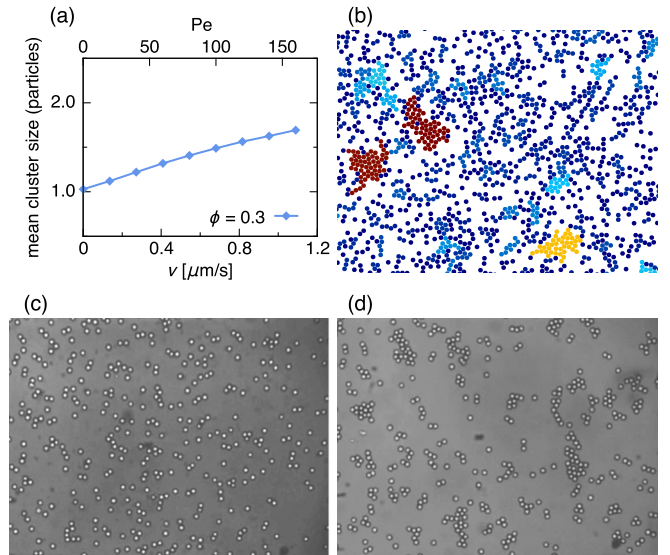
FIG. 3 (color online). Simulation results for the clustering of purely repulsive discs at area fraction $\phi = 0.3$: (a) Mean cluster size as a function of swimming speed v. (b) Snapshot for speed Pe = 140 (corresponding to $v \simeq 0.95$ μm/s). Clusters with same relative size have the same color. For comparison: snapshots (c) and (d) show the experimental suspension for speeds (c) $v \simeq 0.36$ μm/s and (d) $v \simeq 1.51$ μm/s.
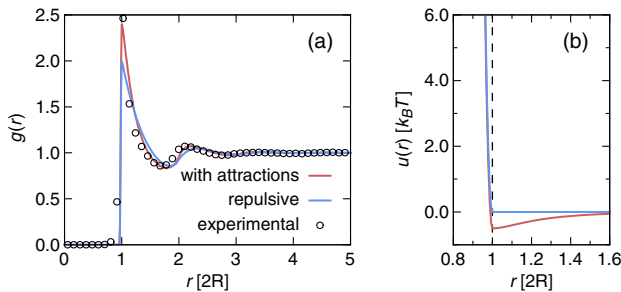
FIG. 2 (color online). (a) Structure of the passive suspension (without illumination): Experimental pair distribution function $g(r)$ at packing fraction $\phi \simeq 0.37$ and simulation results employing the potential Eq. (3) for $\lambda = 0$ (repulsive) and $\lambda = 0.5k_BT$ (slight attractions). (b) Corresponding pair potentials.

In the simulations, clusters finally merge into a single big cluster. This cluster is not static but it is constantly changing its shape while particles are exchanged between the cluster and the diluted phase.

As a geometrical order parameter for the transition, we use the average fraction $P = \langle N_{lc} \rangle / N$ of particles in the largest cluster. In one configuration, N_{lc} is the number of particles that are part of the largest cluster. For the experimental data, we actually add together the size of all clusters larger than $N/10$ particles since we expect all big clusters to finally merge. We only observe the coalescence of smaller clusters and not that a larger cluster breaks up. The order parameter is plotted in Fig. 4(a) as a function of the swimming speed v. At some critical speed it shows a transition from the disordered fluid into the ordered phase, wherein the largest cluster occupies a finite fraction of the system. The ordered state is thus reached by *increasing* the driving strength. The critical speed is shifted to lower values at higher densities. The transition occurs in the experiments already at densities that are lower than what is predicted in the simulations. For the highest experimental density $\phi \simeq 0.36$, the critical speed agrees quite well with the simulations.

What is the mechanism of the cluster formation? Of course, clusters also form in equilibrium systems if attractions between particles are present. For large enough attraction, the gain of energy overcomes the loss of entropy and the suspension separates into a dense liquid or solid,
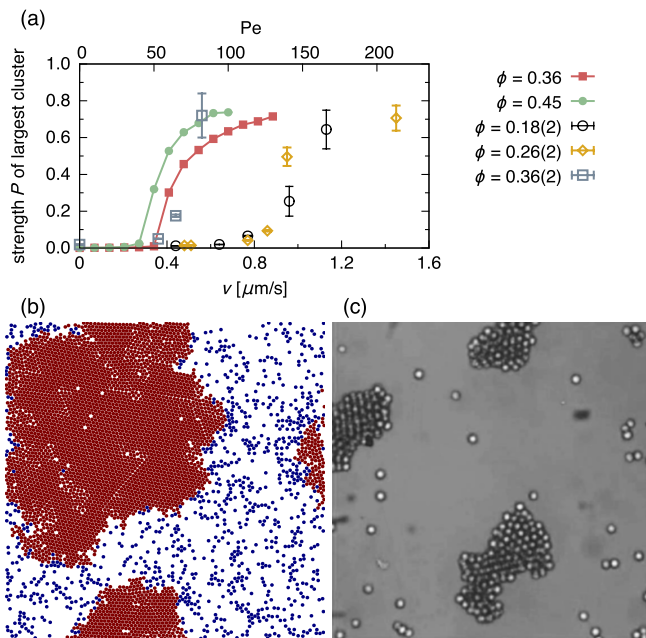
and a dilute gas phase. Thermodynamically stable cluster fluids generally require long-ranged repulsion (e.g., charged particles) together with short-ranged attraction [34] (however, stable cluster fluids in colloidal suspensions have been reported also in the absence of long-ranged repulsion [35]). Because in our experiments we have used carbon instead of a metal as coating material for the Janus particles, we have largely reduced attraction-driven aggregation of particles due to short-ranged van der Waals forces [36]. Moreover, phoretic attractions as well as alignment interactions can be neglected for the experimental conditions used, see the Supplemental Material [31].

To further investigate the clustering mechanism, we have repeated the experiments using larger particles with radius $R \simeq 4$ μm, which allow us to resolve the caps and thus the projected orientations of particles (dynamics is also much slower, which is why for measurements we have employed smaller particles). Figure 5(a) shows consecutive snapshots of a single cluster. Note that the orientations along the rim mostly point inwards. One particle with an outward orientation leaves the cluster while another particle attaches. The emerging physical picture is thus that of a simple self-trapping mechanism, see Fig. 5(b): Two or more particles that collide head-on are blocked due to the persistence of their orientations. Hence, a particle situated in the rim of the cluster has to wait a time $\sim 1/D_r$ until rotational diffusion points its orientation outward to become free again. While the time to leave the cluster is independent of the swimming speed v, a larger swimming speed implies a larger probability for other particles to collide with the cluster, leading to its growth. The size of clusters is determined by the flux balance of incoming and outgoing particles.

(a)

FIG. 4 (color online).   Phase separation: (a) Relative mean size P of the largest cluster as a function of swimming speed v. Shown are experimental results (open symbols) and simulation results (closed symbols). (b) Simulation snapshot of the separated system at $\phi = 0.5$ and speed Pe = 100. (c) Experimental snapshot at $\phi \simeq 0.25$ and $v \simeq 1.45$ μm/s.
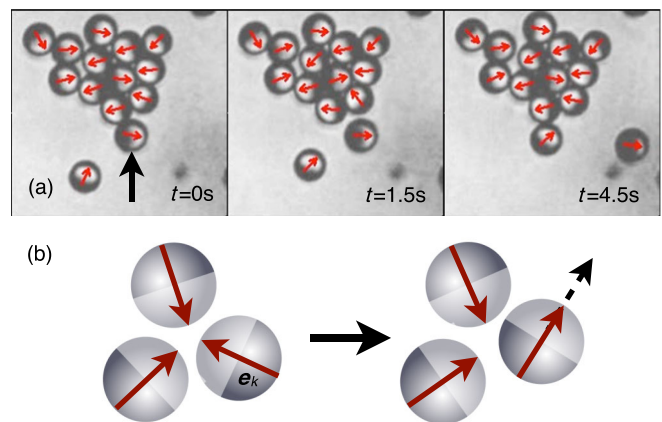

FIG. 5 (color online).   (a) Consecutive close-ups of a cluster, where we resolve the projected orientations (arrows) of the caps. Particles along the rim mostly point inwards. The snapshots show how the indicated particle towards the bottom (left) leaves the cluster (center) and is replaced by another particle (right). (b) Sketch of the self-trapping mechanism: for colliding particles to become free, they have to wait for their orientations to change due to rotational diffusion and to point outwards.

P H Y S I C A L   R E V I E W   L E T T E R S

To summarize, we have presented experimental results for a colloidal suspension of Janus particles that are self-propelled through the heating of a carbon-coated hemisphere in a near-critical binary mixture of water and lutidine. At low densities, we observe the emergence of dynamical clusters. The mean cluster size increases approximately linearly with the propulsion speed in agreement with previous work using catalytic swimmers [10]. At higher densities, the suspension separates into big clusters surrounded by a dilute phase of free swimmers. Both phenomena are captured qualitatively by Brownian dynamics simulations of a minimal model without any alignment interaction and neglecting hydrodynamics.

[1] D. Chandler, *Introduction to Modern Statistical Mechanics* (Oxford University Press, Oxford, 1987).
[2] C. Van den Broeck, J. M. R. Parrondo, and R. Toral, Phys. Rev. Lett. **73**, 3395 (1994).
[3] F. Sagués, J. M. Sancho, and J. García-Ojalvo, Rev. Mod. Phys. **79**, 829 (2007).
[4] D. Helbing, I. J. Farkas, and T. Vicsek, Phys. Rev. Lett. **84**, 1240 (2000).
[5] R. Golestanian, T. B. Liverpool, and A. Ajdari, Phys. Rev. Lett. **94**, 220801 (2005).
[6] Y. Hong, N. M. K. Blackman, N. D. Kopp, A. Sen, and D. Velegol, Phys. Rev. Lett. **99**, 178103 (2007).
[7] J. R. Howse, R. A. L. Jones, A. J. Ryan, T. Gough, R. Vafabakhsh, and R. Golestanian, Phys. Rev. Lett. **99**, 048102 (2007).
[8] H.-R. Jiang, N. Yoshinaga, and M. Sano, Phys. Rev. Lett. **105**, 268302 (2010).
[9] J. Palacci, C. Cottin-Bizonne, C. Ybert, and L. Bocquet, Phys. Rev. Lett. **105**, 088304 (2010).
[10] I. Theurkauff, C. Cottin-Bizonne, J. Palacci, C. Ybert, and L. Bocquet, Phys. Rev. Lett. **108**, 268303 (2012).
[11] G. Volpe, I. Buttinoni, D. Vogt, H.-J. Kümmerer, and C. Bechinger, Soft Matter **7**, 8810 (2011).
[12] I. Buttinoni, G. Volpe, F. Kümmel, G. Volpe, and C. Bechinger, J. Phys. Condens. Matter **24**, 284129 (2012).
[13] J. Palacci, S. Sacanna, A. P. Steinberg, D. J. Pine, and P. M. Chaikin, Science **339**, 936 (2013).
[14] Y. Sumino, K. H. Nagai, Y. Shitaka, D. Tanaka, K. Yoshikawa, H. Chaté, and K. Oiwa, Nature (London) **483**, 448 (2012).
[15] K. Drescher, K. C. Leptos, I. Tuval, T. Ishikawa, T. J. Pedley, and R. E. Goldstein, Phys. Rev. Lett. **102**, 168101 (2009).
[16] K. Drescher, J. Dunkel, L. H. Cisneros, S. Ganguly, and R. E. Goldstein, Proc. Natl. Acad. Sci. U.S.A. **108**, 10 940 (2011).
[17] F. Peruani, J. Starruß, V. Jakovljevic, L. Søgaard-Andersen, A. Deutsch, and M. Bär, Phys. Rev. Lett. **108**, 098102 (2012).
[18] A. Cavagna, A. Cimarelli, I. Giardina, G. Parisi, R. Santagati, F. Stefanini, and M. Viale, Proc. Natl. Acad. Sci. U.S.A. **107**, 11 865 (2010).
[19] T. Vicsek, A. Czirók, E. Ben-Jacob, I. Cohen, and O. Shochet, Phys. Rev. Lett. **75**, 1226 (1995).
[20] H. H. Wensink, J. Dunkel, S. Heidenreich, K. Drescher, R. E. Goldstein, H. Löwen, and J. M. Yeomans, Proc. Natl. Acad. Sci. U.S.A. **109**, 14 308 (2012).
[21] T. Vicsek and A. Zafeiris, Phys. Rep. **517**, 71 (2012).
[22] V. Narayan, S. Ramaswamy, and N. Menon, Science **317**, 105 (2007).
[23] J. Deseigne, O. Dauchot, and H. Chaté, Phys. Rev. Lett. **105**, 098001 (2010).
[24] J. Bialké, T. Speck, and H. Löwen, Phys. Rev. Lett. **108**, 168301 (2012).
[25] Y. Fily and M. C. Marchetti, Phys. Rev. Lett. **108**, 235702 (2012).
[26] G. S. Redner, M. F. Hagan, and A. Baskaran, Phys. Rev. Lett. **110**, 055701 (2013).
[27] J. Tailleur and M. E. Cates, Phys. Rev. Lett. **100**, 218103 (2008).
[28] M. E. Cates and J. Tailleur, Europhys. Lett. **101**, 20 010 (2013).
[29] B. Sabass and U. Seifert, J. Chem. Phys. **136**, 064508 (2012).
[30] J. D. Weeks, D. Chandler, and H. C. Andersen, J. Chem. Phys. **54**, 5237 (1971).
[31] See Supplemental Material at http://link.aps.org/supplemental/10.1103/PhysRevLett.110.238301 for additional data on alignment and phoretic interactions including two movies.
[32] T. Ishikawa and T. J. Pedley, Phys. Rev. Lett. **100**, 088103 (2008).
[33] S. Thutupalli, R. Seemann, and S. Herminghaus, New J. Phys. **13**, 073021 (2011).
[34] F. Sciortino, S. Mossa, E. Zaccarelli, and P. Tartaglia, Phys. Rev. Lett. **93**, 055701 (2004).
[35] P. J. Lu, J. C. Conrad, H. M. Wyss, A. B. Schofield, and D. A. Weitz, Phys. Rev. Lett. **96**, 028306 (2006).
[36] J. N. Israelachvili, *Intermolecular and Surface Forces* (Academic Press, Amsterdam, 1992), 2nd ed.